

experimental results prior to publication, and David M. Bishop for sending them the  $HD^+$  potential-energy curve. One of us (P.R.C.) thanks the A. P. Sloan Foundation for a fellowship.

†This work was supported by National Science Foundation Grant No. CHE74-17494-A01.

<sup>1</sup>W. H. Wing, G. A. Ruff, W. E. Lamb, Jr., and J. J. Spezeski, *Phys. Rev. Lett.* **36**, 1488 (1976).

<sup>2</sup>D. M. Bishop, *Phys. Rev. Lett.* **37**, 484 (1976).

<sup>3</sup>K. B. Jefferts, *Phys. Rev. Lett.* **23**, 1476 (1969).

<sup>4</sup>A. Dalgarno, T. N. L. Patterson, and W. B. Somerville, *Proc. Roy. Soc. London, Ser. A* **259**, 100 (1960).

<sup>5</sup>S. K. Luke, *Astrophys. J.* **156**, 761 (1969), and references contained therein.

<sup>6</sup>P. M. Kalaghan and A. Dalgarno, *Phys. Lett.* **38A**, 485 (1972).

<sup>7</sup>J. J. Tortorelli and J. E. Harriman, University of Wisconsin Theoretical Chemistry Institute Report No. WIS-TCI-456, 1971 (unpublished).

<sup>8</sup>D. M. Bishop and R. W. Wetmore, *J. Mol. Spectrosc.* **26**, 145 (1973).

### Stability Limitations on High-Beta Tokamaks\*

A. M. M. Todd, M. S. Chance, J. M. Greene, R. C. Grimm, J. L. Johnson,† and J. Manickam  
*Plasma Physics Laboratory, Princeton University, Princeton, New Jersey 08540*

(Received 24 January 1977)

Magnetohydrodynamic instabilities limit the material that can be contained in a tokamak. The nature of the dangerous kink and ballooning modes is investigated for a typical configuration. In high-beta systems the most dangerous instabilities are ballooning modes that form large convective cells concentrated in regions of unfavorable magnetic field-line curvature.

The flux-conserving tokamak concept<sup>1</sup> has provided a prescription for choosing achievable plasma parameters when rapidly heating a plasma from an easily formed low-pressure configuration. It has been shown that equilibrium considerations do not provide an absolute limit to the maximum pressure that can be contained. Magnetohydrodynamic stability considerations provide such a limit. We study this problem numerically, using the PEST package,<sup>2</sup> by treating a series of equilibria that could be associated with the device<sup>3</sup> being built at the Princeton University Plasma Physics Laboratory.

We choose as our starting point the equilibrium of Fig. 1. The pressure is proportional to  $(\Psi_b - \Psi)^2$  with  $\Psi_b$  the poloidal flux at the plasma boundary. The safety factor  $q \equiv d\Phi/d\Psi$ , with  $\Phi$  the toroidal flux, increases from 1.04 at the axis to 3.77 at the boundary. The plasma, with aspect ratio  $R/a = 4.6$ , where  $R$  is the distance from the major axis to the magnetic axis and  $\pi a^2$  the cross-sectional area of the plasma surface, is supported by currents in external poloidal field coils that create a favorable field index throughout the plasma. The fusion-power-averaged pressure is

$$\beta^* = 2\mu_0 \left( \int p^2 dV / V \right)^{1/2} B_0^{-2} = 1.6\% \quad (1)$$

for this configuration. Other commonly used

pressure averages include

$$\bar{\beta} \equiv 2\mu_0 \int p dV / B_0^2 V = 1.0\%$$

and

$$\beta_p \equiv 4 \frac{\int p dV}{\int (I'V/V') d\Psi} = 2.1,$$

with  $I$  the toroidal current,  $V$  the volume, and  $B_0$  the toroidal field. The difference between  $\beta^*$  and

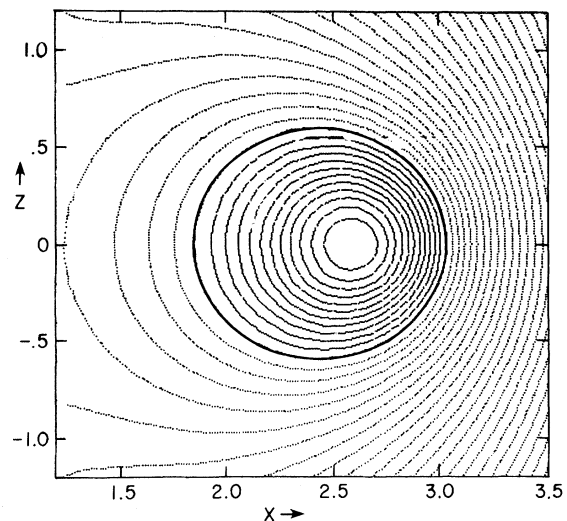
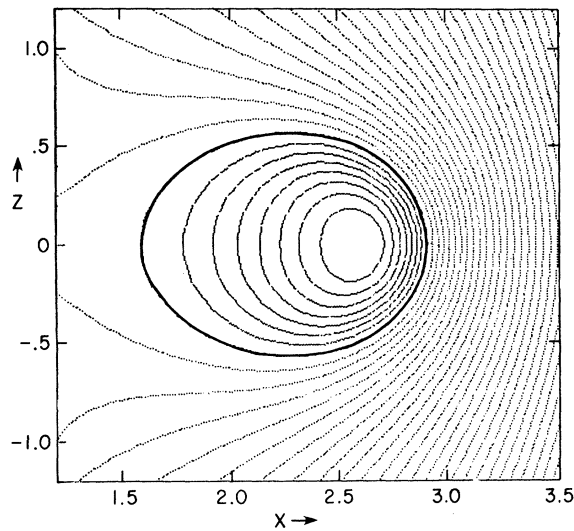


FIG. 1. Flux surfaces for a TFTR configuration with  $\beta^* = 1.6\%$ . The heavy solid curve is the plasma surface.

FIG. 2. Flux surfaces with  $\beta^* = 6.0\%$ .

$\bar{\beta}$  depends strongly on the shape of the pressure distribution.

We consider the effect on this equilibrium of increasing the material pressure, keeping the shape of the pressure distribution, the magnetic fluxes, and the position of the magnetic axis fixed. To prevent the outward shift associated with a pressure increase, we raise the current in the poloidal field coils, maintaining the shape of the field. As shown in Fig. 2, which is a plot of the flux surfaces when  $\beta^* = 6.0\%$  and  $\beta_p = 4.2$ , the separatrix in the vacuum region approaches the plasma as the pressure is increased. As it comes close, the change in shape of the magnetic surfaces modifies their inductance and thus induces a large current in the plasma close to the surface.

We now consider the stability problem. Evaluation of the usual localized instability criteria<sup>4</sup> shows that both ideal and resistive interchange modes should be stable. We investigate nonlocal instabilities using a Galerkin method<sup>2</sup> to find the eigenmodes  $\xi$ . We use finite elements in the  $\Psi$  direction, perform a Fourier analysis in the poloidal and toroidal angles  $\theta$  and  $\varphi$ ,

$$\xi = \sum_{m, l, n} \xi_{m, l, n} \Phi_m(\Psi) \exp i(l\theta - n\varphi),$$

and treat the different  $n$  modes separately.

The axisymmetric modes with  $n = 0$  are stable. This should be expected since the shape of the externally imposed field was tailored carefully to avoid such instabilities.

Instabilities with  $n = 1$  set in for  $\beta^* > 1.9\%$  as

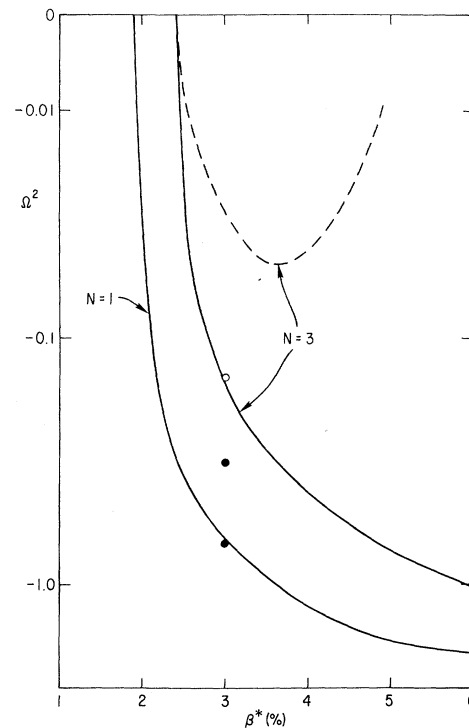


FIG. 3. Instability growth rates on a  $\sinh^{-1} 100\Omega^2$  scale for  $n=1$  and  $n=3$  modes with a free boundary (solid curves) and for  $n=3$  modes with a fixed boundary (dashed curve). The fixed-boundary  $n=1$  mode is stable. The apparent decrease of  $\Omega^2$  for  $\beta^* > 3\%$  in the dashed curve is due to the need for more expansion functions to represent the localization of the ballooning modes. The curves have been prepared with twelve finite elements in  $\Psi$  and 21  $\theta$  components. Convergence studies decrease the onset of the  $n=3$  modes to  $\beta^* \sim 1.9\%$  with more expansion functions needed at higher  $\beta^*$ 's. Three dots, demonstrated results obtained by an extrapolation, are shown at  $\beta^* = 3\%$ . Each one represents the convergence limit point corresponding to the curve above it. It is interesting to note that the growth rate of the  $n=3$  mode is not substantially affected by the presence of a conducting wall.

shown in Fig. 3. The growth rate is normalized to the poloidal Alfvén time. The projection of the displacement vector onto a constant  $\varphi$  plane is shown in Fig. 4. The  $l=1$  component dominates at the axis; higher  $l$ 's emerge near the rational surfaces where their perturbed fields are small, i.e., where  $|l - nq| < 1$ , and thus the  $l=4$  mode is largest at the surface. The modes twist with the field lines in going around the torus with largest amplitude on the outside. The system is found to be stable to this mode when the plasma surface is held fixed. Over all, this mode has the character of an  $l=4$  kink with an enhanced

and deepened vortex on the outer side of the plasma column.

Higher- $n$  modes set in for somewhat larger  $\beta^*$ 's as shown for  $n=3$  in Fig. 3. Holding the plasma boundary fixed decreases the growth rate but does not eliminate the instability. A typical displacement vector is shown in Fig. 5. The instability assumes the form of vortices which are stronger on the outside of the plasma column.

To understand the importance of these modes, it is useful to consider the potential energy associated with small distortions from equilibrium<sup>2</sup>:

$$2\delta W = \int d\tau \left[ \vec{Q}_\perp^2 + \left( \vec{Q}_\parallel - \vec{B} \frac{\vec{\xi} \cdot \nabla p}{B^2} \right)^2 + \gamma p (\nabla \cdot \vec{\xi})^2 + \frac{\vec{J} \cdot \vec{B}}{B^2} \vec{B} \times \vec{\xi} \cdot \vec{Q} - 2\vec{\xi} \cdot \nabla p \vec{\xi} \cdot \vec{\kappa} \right], \quad (2)$$

with  $\vec{Q} \equiv \nabla \times (\vec{\xi} \times \vec{B})$  the perturbed field and  $\vec{\kappa}$  the field-line curvature. The first term measures the field-line tension associated with shear-Alfvén waves. Marginally unstable modes have  $\nabla \cdot \vec{\xi}_\perp \approx -2\vec{\xi} \cdot \vec{\kappa}$  to eliminate the second term, associated with fast magnetosonic waves, and  $\nabla \cdot \vec{\xi} \approx 0$ , thereby removing the slow waves associated with the third term. Kink modes<sup>5</sup> are driven primarily by the interaction of the perturbed field with the force-free part of the current, the fourth term. The toroidal field provides a large curvature of order  $1/R$ , unfavorable on the outside of the plasma and favorable on the inside. The outward shift of the magnetic axis weights the inside and stabilizes the interchange modes<sup>6</sup> with  $\vec{\xi} \cdot \nabla \Psi$  constant along the field lines. Relaxing this constraint on  $\vec{\xi} \cdot \nabla \Psi$  allows the unfavorable curvature to drive the modes unstable despite the increase in the magnitude of the  $Q_\perp^2$  term.<sup>7</sup> The shear term,  $Q_\perp^2 \approx (\vec{B} \cdot \nabla \xi_\perp)^2 \approx (B/qR)^2 \xi^2$ , with  $qR$  an approximate connection length, and the curvature term,  $2\vec{\xi} \cdot \nabla p \vec{\xi} \cdot \vec{\kappa} \approx 2(p/a)\xi^2/R$ , balance when  $\beta^* \lesssim a/q^2R \approx 1.5\%$  for our parameters. The enve-

lopes of the curves in Fig. 6, where  $\xi \cdot \nabla \Psi$  is plotted as a function of  $\theta$ , display the ballooning character of the modes. These effects augment the driving forces for kink modes to establish an upper limit on  $\beta^*$ .<sup>8</sup>

The ballooning modes, illustrated by the fixed-wall  $n=3$  case, provide a mechanism for moving plasma from the center to the outer surface. They appear to be described by a quasimode formulation.<sup>9</sup> Thus, it is reasonable to expect that the instability will develop nonlinearly on a resistive instability time scale. These modes, therefore, pose a severe limitation on the achievable beta.

The low  $\beta^*$ 's found here are due to the particular aspect ratio, safety factor, and cross section, which were chosen to ensure stability with respect to axisymmetric and kink modes. A more rigorous analysis would include the destabilizing effects associated with the force-free currents and the stabilization associated with nonlocal effects and the fact that the connection length is

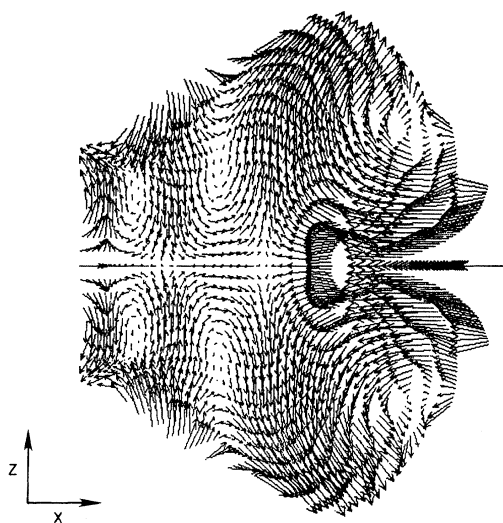


FIG. 4. Projection of the displacement vector for the free-boundary  $n=1$  mode at  $\beta^*=3.0\%$ .

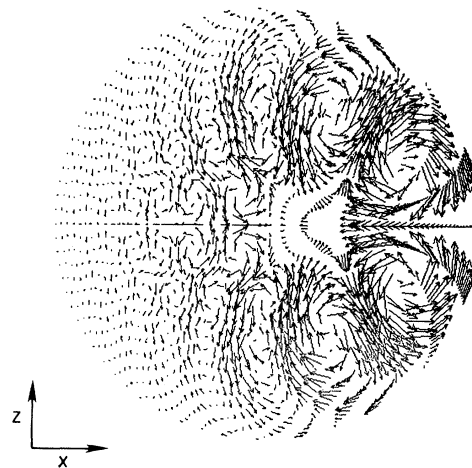


FIG. 5. Displacement vector for the fixed-boundary  $n=3$  mode at  $\beta^*=3.0\%$ .

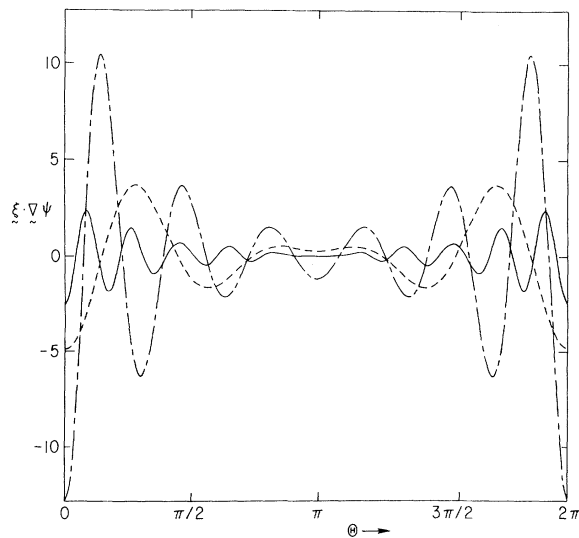


FIG. 6. The displacement  $\xi \cdot \nabla \Psi$  as a function of the poloidal angle on surfaces with  $\Psi/\Psi_b = \frac{1}{12}$  (dashed curve),  $\Psi/\Psi_b = \frac{1}{2}$  (broken curve), and  $\Psi/\Psi_b = \frac{11}{12}$  (solid curve) for the fixed-wall  $n=3$  mode at  $\beta^* = 3.0\%$ .

less than  $qR$ . Clearly, a better understanding of these instabilities is essential.

We appreciate the interest shown by H. P. Furth, P. H. Rutherford, M. Okabayashi, and Y. Hsieh.

\*This work was supported by the U. S. Energy Research and Development Administration Contract No. E(11-1)-3073.

†On loan from Westinghouse Research Laboratories.

<sup>1</sup>J. M. Clarke and D. J. Sigmar, *Phys. Rev. Lett.* **38**, 70 (1977).

<sup>2</sup>R. C. Grimm, J. M. Greene, and J. L. Johnson, *Methods in Computational Physics* (Academic, New York, 1976), Vol. 16, p. 253.

<sup>3</sup>Tokamak Fusion Test Reactor (TFTR) Final Conceptual Design Report, Princeton University Plasma Physics Laboratory and Westinghouse Electric Corporation Fusion Power Systems Department Report No. PPPL-1275, PH, R-001, February 1976 (unpublished).

<sup>4</sup>A. H. Glasser, J. M. Greene, and J. L. Johnson, *Phys. Fluids* **18**, 875 (1975).

<sup>5</sup>M. D. Kruskal, J. L. Johnson, M. B. Gottlieb, and L. M. Goldman, *Phys. Fluids* **1**, 421 (1958).

<sup>6</sup>J. M. Greene and J. L. Johnson, *Plasma Phys.* **10**, 729 (1968).

<sup>7</sup>H. P. Furth, J. Killeen, M. N. Rosenbluth, and B. Coppi, in *Proceedings of a Conference on Plasma Physics and Controlled Nuclear Fusion Research, Culham, England, 1965* (International Atomic Energy Agency, Vienna, Austria, 1966), Vol. 1, p. 103.

<sup>8</sup>J. P. Freidberg, J. P. Goedbloed, W. Grossmann, and F. A. Haas, in *Proceedings of the Fifth International Conference on Plasma Physics and Controlled Nuclear Fusion Research, Tokyo, Japan, 1974* (International Atomic Energy Agency, Vienna, Austria, 1975), Vol. 1, p. 505.

<sup>9</sup>K. V. Roberts and J. B. Taylor, *Phys. Fluids* **8**, 315 (1965).

## Magnetohydrodynamic Stability of Flux-Conserving Tokamak Equilibria\*

Glenn Bateman and Y.-K. M. Peng

Oak Ridge National Laboratory, Oak Ridge, Tennessee 37830

(Received 7 February 1977)

Large-scale magnetohydrodynamic instabilities of flux-conserving tokamak equilibria are studied computationally. Stable equilibria are found with up to 5% average  $\beta$ . As  $\beta$  is increased, the observed instabilities take on a strong ballooning character, concentrating near the outer edge of the torus with a mix of poloidal harmonics.

For the purpose of controlled thermonuclear fusion, it is desirable to build a tokamak with the highest possible energy density relative to the confining magnetic field—the highest possible average  $\beta$ ,

$$\langle \beta \rangle \equiv 2\mu_0 \langle p \rangle / B_{\text{tor}}^2,$$

where  $\langle p \rangle$  is the pressure averaged over the plasma volume and  $B_{\text{tor}}$  is the vacuum toroidal magnetic field at the geometric center of the plasma. As the plasma pressure in a tokamak is raised, by neutral beam injection, for example, poloidal

currents play a progressively larger part in providing the radial force balance to confine the plasma; thus there is an increase in the poloidal  $\beta$ ,

$$\beta_{\text{pol}} \equiv 2\mu_0 \langle p \rangle / (\oint dl B_{\text{pol}} / \oint dl)^2,$$

where the integral is performed around the plasma boundary. In addition, the vertical magnetic field which restrains the plasma from expanding along the major radius of the torus must be increased.<sup>1</sup> For arbitrarily chosen equilibrium profiles it is theoretically predicted<sup>2</sup> that the vertical field will tend to cancel the poloidal magnet-